

Laboratory study of differential rotation in a convective rotating layer

VLADIMIR BATALOV, ANDREY SUKHANOVSKY † and PETER FRICK
Institute of Continuous Media Mechanics, Korolyov Street 1, Perm, 614013, Russia

(Received 00 Month 200x; in final form 00 Month 200x)

The evolution of a large-scale azimuthal velocity field in a rotating cylindrical layer of fluid (radius 150 mm, depth 30 mm, free upper surface) with meridional convective circulation was studied experimentally. Two cases were considered: direct circulation provided by a rim heater at the periphery and indirect circulation provided by a central heater. The heating rate is characterized by the Grasshoff number Gr_f defined through the density of the heat flux. The detailed 3D structure of the mean large-scale velocity field is reconstructed using the PIV technique for $10^5 < Gr_f < 4 \cdot 10^7$. It was shown that the energy of meridional circulation grows with the Grasshoff number as $\sqrt{Gr_f}$ in both directions of circulation. Due to the action of the Coriolis force the meridional flow results in differential rotation. Differential rotation is characterized by the mean values of radial and vertical gradients of azimuthal velocity. Strong negative mean radial gradient which grows with the Grasshoff number is provided by direct circulation. In the case of indirect circulation a pronounced negative gradient arises at moderate Grasshoff number. The behavior of the mean vertical gradient is quite different: a positive vertical gradient grows logarithmically with Grasshoff number under direct circulation, whereas a weak negative gradient characterizes the indirect circulation. This difference follows from the structure of the flow – the direct circulation provides a large cyclonic area localized above the anticyclonic flow, while indirect circulation leads to a strong separation of these two areas in the radial direction (the central part is occupied by the cyclonic flow and the periphery by the anticyclonic flow). Meridional circulation leads to substantial variation of the integral angular momentum. Direct circulation results in the growth of the integral angular momentum and indirect circulation causes it to decrease. At the same heating power, the increase of angular momentum at direct circulation is much stronger than its decrease at indirect circulation.

1 Introduction

All cosmic bodies rotate to a greater or lesser extent. The evolution of these bodies (excluding catastrophic events) proceeds under a very slow variation of the global angular momentum. However, if the cosmic object is gaseous or liquid (galaxies, stars) or includes liquid and/or gaseous shells (planets) the averaged large-scale azimuthal velocity field becomes essentially inhomogeneous in both the radial and meridional directions. The deviation from the solid body rotation is called differential rotation (DR).

DR plays a crucial role in the generation of cosmic magnetic fields (Zeldovich *et al.* 1983) and has created considerable interest in investigating DR in electrically conducting cosmic media - such as stellar convective zones, liquid planet cores and galactic disks (Kleeorin & Rogachevskii 2006, Kitchatinov & Rudiger 2007). The study of DR in nonconducting rotating (spherical) layers has primarily been motivated by atmospheric research because DR is a part of the global atmospheric circulation that determines climate formation (Williams 1968). For the most part, large-scale circulation in the atmosphere is caused by the horizontal temperature gradient, i.e., it has a convective nature. This strongly motivated laboratory experiments on convection in rotating vessels (cylinders or annuli) (Highnett *et al.* 1981, Boubnov & Golitsyn 1995). The first generation of laboratory experiments primarily intended to reproduce the Hadley cell (or direct meridional circulation) by realizing a convective flow in rotating annuli or flat cylinders heated at the periphery and cooled in the center (Hide 1958, Fultz & Kaiser 1971). Wave-transition spectra and vacillations were studied by Spence & Fultz (1977). Interest in DR in this configuration has been heightened by the discovery of so-called super-rotation in the atmosphere of Venus (Belton *et al.* 1976) - the existence in the high atmosphere of very fast latitudinal circulation, which exceeds by about 60 times the rotational velocity of the surface (the rotation period is about four days versus 243 days of the Venus astronomical day). The problem of super-rotation is directly linked with processes of angular momentum diffusion

† Corresponding author: san@icmm.ru

and transport in planetary atmospheres. It was proposed by Gierasch (1975) that Venus super-rotation is maintained by angular momentum transport provided by meridional circulation. Some mechanisms, which may contribute to the development of a strong differential rotation were proposed (Shubert & Young 1970, Rossow 1983). Comprehensive review of different quasy-axisymmetric models of planetary atmospheres can be found in (Read 1986).

The first experimental attempt to quantitatively analyze meridional transport of angular momentum in the rotating layer of fluid in the case of direct meridional circulation was realized by Spence & Fultz (1977), however, integral characteristics such as overall angular momentum were not studied. Numerical simulations for a similarly stated problem using different boundary conditions were presented by Williams (1967, 1968) and showed good agreement with experimental results from Spence & Fultz (1977).

Properties of angular momentum budget and super-rotation of axisymmetric thermally-driven circulations in a rotating cylindrical fluid annulus were studied numerically by Read (1986). Angular momentum diffusion due to molecular viscosity was examined and was found to be very important for super-rotating flow formation in a system with stress-free top and side boundaries and a non-slip bottom. It was shown that global super-rotation is connected with direct meridional circulation.

An opposite situation to the direct meridional cell is the indirect cell, usually produced in a rotating layer of fluid by heating at the center. Mainly, it was studied in the context of another atmospheric problem concerning the generation of intense large-scale vortices. Laboratory modeling of these typhoon-like vortices was made (Bogatyrev 1990, Bogatyrev & Smorodin 1996, Bogatyrev *et al.* 2006). These studies were concentrated on cyclonic vortex formation and its evolution. A qualitative experimental study of convective flow driven by a finite-sized circular heating plate at the bottom of a horizontal fluid layer, both with and without background rotation, was carried out by Boubnov & Heijst (1994). The angular momentum budget for an indirect cell was analyzed by Read (1986) and it was shown that indirect circulation resulted in local and/or global sub-rotation, thereby demonstrating that the change in overall angular momentum essentially depends on the type of meridional circulation.

In this paper, we return to experimental investigation of the convection flow in rotating cylindrical vessels, being motivated by following reasons. First, we examine the differential rotation problem in the rotating layer heated at the periphery or center from a uniform viewpoint, paying special attention to the integral characteristics of differential rotation. Second, our experiment concerns the *shallow* layer of fluid. And third, we obtain the full structure of meridional and azimuthal velocity fields exploiting the potentialities of the PIV technique (Raffel *et al.* 1983, Xia *et al.* 1976).

We note that our statement of the problem is similar to that made in (Read 1986), except for the aspect ratio and the physical properties of the fluid. Numerical simulations in (Read 1986) were carried out for fluid layers in an annular channel with an aspect ratio close to unity, whereas we studied the cylinder layer (no inner wall) with a fixed aspect ratio $\varepsilon = h/R = 0.2$ (h - depth of the layer, R - radius of the cylindrical vessel). The Prandtl number for the fluid in (Read 1986) was about 10, and in our study it is about 100.

The structure of the paper is as follows. The experimental set up is described in Sec. 2. The structure of convective flows for direct and indirect meridional cells is represented in Sec. 3 and Sec. 4, respectively. Integral characteristics of DR are described in Sec. 5. Our results are summarized in Sec. 6.

2 Experimental set-up

We studied a convective flow in a flat cylindrical vessel placed on a rotating horizontal table (Fig. 1). The table provides uniform rotation in the angular speed range $0.04 \leq \Omega \leq 0.30 \text{ s}^{-1}$ (with accuracy of $\pm 0.002 \text{ s}^{-1}$). The cylinder radius is $R = 150 \text{ mm}$. The cylinder is made of acrylic plastic, which is transparent to the laser sheet. The fluid is transformer oil, characterized by a high Prandtl number

$$\text{Pr} = \nu/\chi, \quad (1)$$

where ν, χ are the kinematic viscosity and thermal conductivity (for transformer oil, $\text{Pr} = 116$ at 50° C). The layer thickness is constant in all experiments ($h = 30 \text{ mm}$) and the upper surface is free.

Two heaters were installed at the bottom of the vessel (Fig. 1). Heater I is a copper rim 20 mm wide

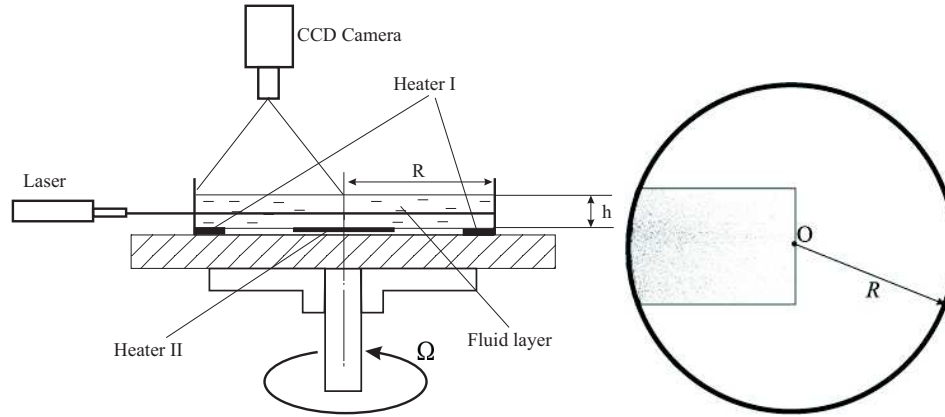


Figure 1. Left panel - scheme of the laboratory set-up; Right panel (view from above) - zone of horizontal velocity measurements where a typical (here inverted) PIV image is shown. O - axis of rotation.

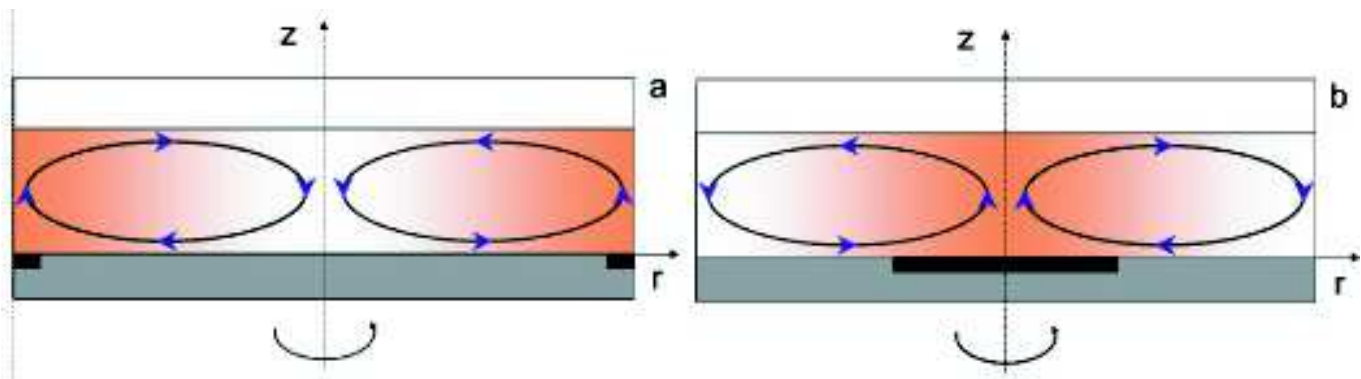


Figure 2. Sketch of meridional circulation, initiated by peripheral heater I (direct circulation - a) and by central heater II (indirect circulation - b). The heaters are shown by black boxes.

Table 1. Experimental parameters

Heater	P, Wt	Ω	E	Gr_f	Pr
I	14.2	0.069	0.118	$1.4 \cdot 10^5$	209
I	35.3	0.069	0.082	$7.7 \cdot 10^5$	151
I	55.1	0.069	0.053	$2.9 \cdot 10^6$	101
I	73.8	0.069	0.044	$5.8 \cdot 10^6$	85
I	95.8	0.069	0.032	$1.4 \cdot 10^7$	63
II	6.9	0.069	0.137	$1.1 \cdot 10^5$	226
II	14.3	0.069	0.104	$4.1 \cdot 10^5$	187
II	24.7	0.069	0.075	$1.4 \cdot 10^6$	137
II	55.8	0.069	0.044	$9.3 \cdot 10^6$	84
II	95.7	0.069	0.032	$3.0 \cdot 10^7$	63

placed at the periphery of the cylinder. This heater provided the direct meridional circulation as shown in Fig. 2(a). Heater II is a copper cylinder of radius 52 mm, installed in the center of the vessel and coinciding with the axes of rotation. The heating near the rotation axes (polar heating) provides circulation in the opposite direction (indirect circulation, Fig. 2(b)). Both heaters operate from a DC power supply. The room temperature is kept constant, and cooling is provided by the heat exchange on the free surface. It takes about two hours to obtain a steady-state temperature regime.

The velocity field measurements were made for steady state regimes by a 2D particle image velocimetry (PIV) system, "Polis", manufactured by the Institute of Thermophysics (Novosibirsk). A CCD camera is placed above the rotating vessel in the laboratory coordinate system as shown in Fig. 1. The measurements

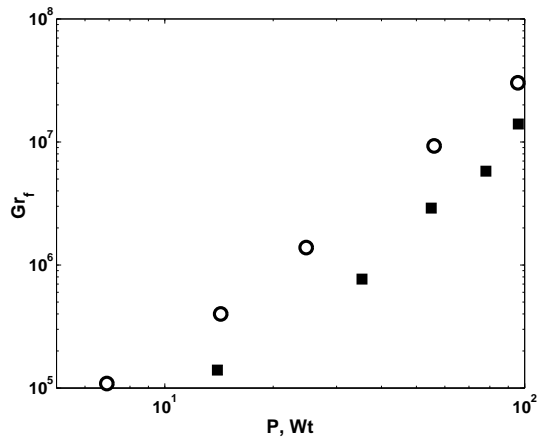


Figure 3. Grasshoff number versus heating power: squares – heater I, circles – heater II, $\Omega = 0.069s^{-1}$.

are carried out in a confined area of the vessel, but the rotation provided averaging for the entire horizontal cross-section. The area of velocity measurements is shown in Fig. 1. PIV measurements are done at horizontal cross-sections for $4 \leq z \leq 28, \text{mm}$ in 2 mm steps (the cylindrical coordinate system (r, ϕ, z) is used). We focused on flow motions in the rotating frame, and for this purpose the velocity field of solid-body rotation was subtracted and all velocity fields and flow characteristics, described as follows, are related to the motions in the rotating frame. The time-averaged velocity fields consist of 41×30 vectors and were averaged over 100 instant velocity fields. Then time-averaged horizontal velocity components v_ϕ and v_r are averaged along the coordinate ϕ and the mean velocity fields at vertical cross-section are reconstructed. The domain of PIV measurements is restricted by the boundary layers, where the velocity field reconstruction is hampered by optical distortions caused by strong temperature gradients near the heaters and/or by high velocity gradients. These boundary layers are shown in white in figures given below. The PIV velocity measurements were accurate to within 5%.

Two main factors are responsible for DR in the flows under discussion – convection and rotation. To characterize the intensity of convective flows, we use the Grasshoff number Gr_f , defined in terms of layer depth h and heat flux density $q = P/S_h$ (P is the power of the heater and S_h is the heater’s surface area)

$$Gr_f = \frac{g\beta h^4 q}{c\rho\chi\nu^2}, \tag{2}$$

where g is the gravitational acceleration, β is the coefficient of thermal expansion, c is the thermal capacity, and ρ is the density. Because the fluid characteristics depend on temperature (particularly viscosity) and the mean temperature of the layer is a function of the heating power P , Gr_f is a nonlinear function of P . In Fig. 3 Gr_f versus P is plotted on a log-log scale for both heaters. This graph shows that the dependence is even stronger than a squared relationship, and is similar for both heaters.

As a non-dimensional characteristic of rotation we use the Ekman number

$$E = \frac{\nu}{2\Omega h^2} \tag{3}$$

because formation of DR strongly depends on angular momentum exchange in viscous boundary layers. The values of parameters for all experiments are given in Table 1.

3 Direct circulation

In laboratory models of general atmospheric motions, the direct meridional circulation is usually provided by heating the outer (peripheral) parts of cylindrical vessels (Highnett *et al.* 1981, Hide 1958, Fultz & Kaiser 1971, Spence & Fultz 1977). The generated flow can be considered as a rough model of

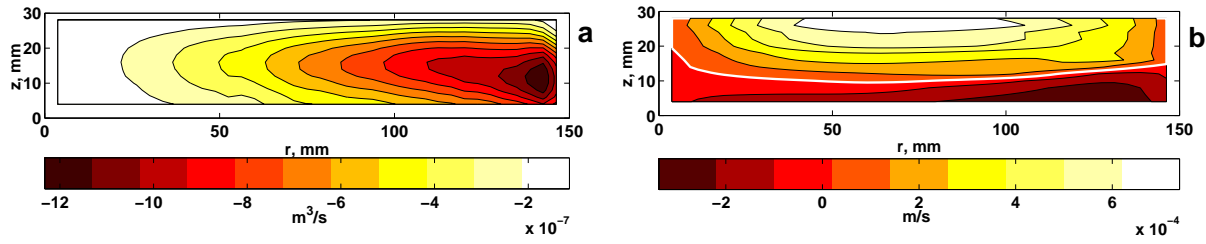


Figure 4. (Color online.) Stream function of the meridional mean velocity field (a) and mean azimuthal velocity field (b) for direct circulation at $Gr_f = 1.4 \cdot 10^5$, $E = 0.118$. Positive values of v_ϕ are related to the cyclonic flow and negative- to the anticyclonic flow. The border between the cyclonic and anticyclonic motion is shown by the white line.

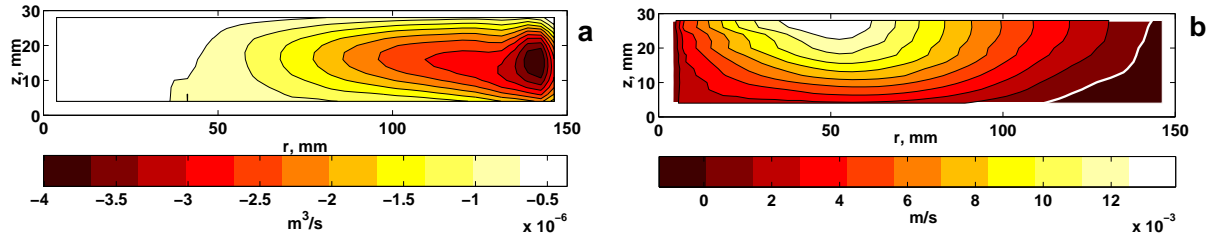


Figure 5. (Color online.) Stream function of the meridional mean velocity field (a) and mean azimuthal velocity field (b) for direct circulation at $Gr_f = 1.4 \cdot 10^7$, $E = 0.032$.

atmospheric meridional circulation (the Hadley cell) in which the role of latitudinal variation of Ω_z is neglected (Williams 1968). In our experiments, a horizontal temperature difference is maintained by heating the periphery of the bottom and by natural cooling at the free upper surface. We studied the evolution of the direct meridional flow structure with variation in the heating power and the contribution of the meridional toroidal cell to differential rotation. All measurements are made for a fixed rotation speed, $\Omega = 0.069s^{-1}$.

At weak heating the meridional flow has the structure shown in Fig. 2(a). The stream function ψ , defined for the mean flow in the radial cross-section as

$$\partial_z \psi = -rv_r, \quad \partial_r \psi = rv_z, \quad (4)$$

where v_r is the radial velocity component and v_z is the vertical velocity component, is shown in Fig. 4,a for $Gr_f = 1.4 \cdot 10^5$, $E = 0.118$. The meridional cell occupies the whole layer providing an inward (polarward) radial flow in the upper part and an outward flow in the lower part of the layer. The center of the cell (the maximum of the stream function) is localized close to the cylinder wall, where the heater produces an intensive upward flow.

Formation of differential rotation in such a system can be described as follows. At first, the action of the Coriolis force on the radial flows initiates cyclonic (prograde) azimuthal flow in the upper layer and anticyclonic (retrograde) flow near the bottom. Then, angular momentum transport provided by meridional circulation and angular momentum diffusion due to molecular viscosity lead to the steady-state regime shown in Fig. 4(b). The maximum cyclonic velocity is located near the free surface at $r \approx R/2$, and the maximum anticyclonic velocity is located near the bottom, shifted to the outer side.

The growth of Gr_f intensifies the meridional flow (see Fig. 5(a), where the stream function for $Gr_f = 1.4 \cdot 10^7$ is shown). Now, the main meridional convective cell is pressed more to the periphery of the rotating layer. The azimuthal velocity field in Fig. 5(b) shows an absolute dominance of the cyclonic zonal circulation, and the anticyclonic motion survives only in a small area near the wall. The maximum of the cyclonic flow is shifted polarward compared to its position in the previous case (Fig. 4), but the intensity of this flow grows dramatically (the maximal azimuthal velocity grows from 0.7mm/s to 13 mm/s). The ratio of the maximum of the cyclonic flow velocity to the velocity of the underlying solid border is more than 3 (compared to 0.1 in the previous case).

The measured velocity fields are in good qualitative agreement with the numerical simulation of rotating

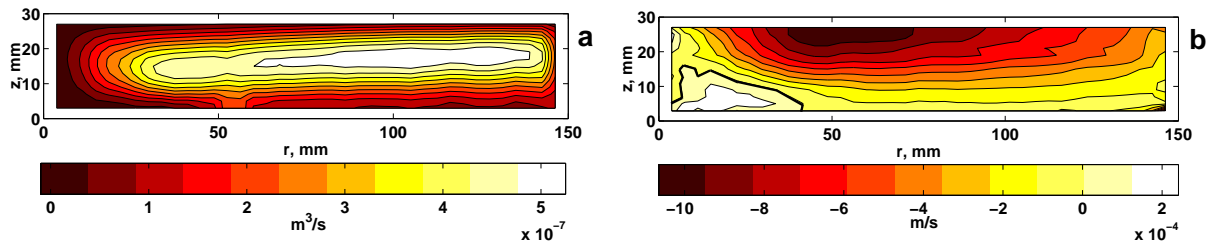


Figure 6. (Color online.) Stream function of the meridional mean velocity field (a) and mean azimuthal velocity field (b) for indirect circulation at $Gr_f = 4.1 \cdot 10^5$, $E = 0.104$. The dashed black line marks the border between the cyclonic and anticyclonic motion.

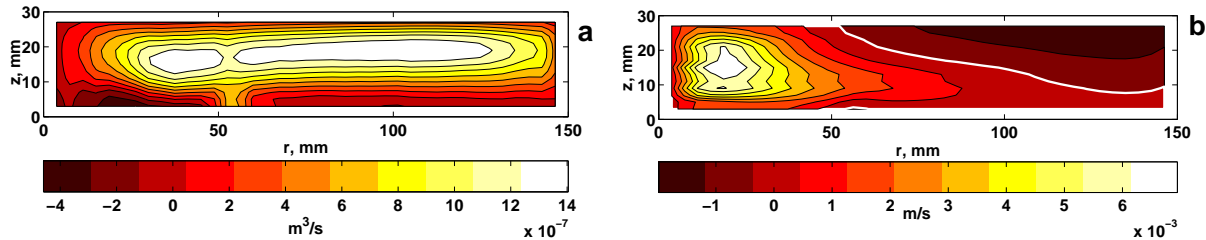


Figure 7. (Color online.) Stream function of the meridional mean velocity field (a) and mean azimuthal velocity field (b) for indirect circulation at $Gr_f = 3.02 \cdot 10^7$, $E = 0.032$. The solid white line marks the border between the cyclonic and anticyclonic motion.

convection in a wide annular gap (Williams 1968). The dominance of cyclonic flow in the layer with a free surface is mainly caused by different boundary conditions on the free surface and at the rigid bottom. In the case with all rigid boundaries cyclonic and anticyclonic flow were essentially balanced (Williams 1968).

4 Indirect circulation

In this section we describe the mean flow induced by heater II, located at the center of the cylinder bottom. Natural convection over the local heat sources with and without background rotation has many geophysical and engineering applications and has been widely studied. Most of these studies were focused on heat transfer measurements and qualitative studies of the flow structure. A systematic study of the dependence of the convective flow regimes on the aspect ratio δ and the Rayleigh number was carried out by Boubnov & Heijst (1994). The aspect ratio was defined as $\delta = D/h$, where D is the *diameter of the heater*. Four domains corresponding to different regimes were defined in the (δ, Ra) plan: I - laminar toroidal cell; II - thermal plumes; III - turbulent flow; and IV - transition regime. Following this classification, all our experiments belong to case III - turbulent flow ($\delta = 3.5$, $1.5 \cdot 10^5 < Ra_h < 6.5 \cdot 10^6$). Here $Ra_h = g\beta\Delta Th^3(\nu\chi)^{-1}$.

The structure of the mean (axisymmetric) flow is determined again by two factors: heating power and frame rotation speed. First, we varied the heating power at a fixed rotational speed ($\Omega = 0.069 \text{ s}^{-1}$). Local heating at the center of the bottom generates vertical and horizontal temperature gradients. The horizontal temperature difference provides an indirect axisymmetric meridional cell (Fig. 2(b)). The flow in the lower part is directed inward, tending to the central bottom region, where the heat source is located. A strong upward flux is formed at the center above the heat source. In the upper layer, the outward flow is directed toward the periphery. The fluid is cooled at the free surface and finally moves downward along the side wall. Fig. 6 shows the mean velocity fields at $Gr_f = 4 \cdot 10^5$. The growth of Gr_f increases the intensity of the meridional flow, but does not appreciably change its structure (compare panels (a) in Fig. 6 and Fig. 7).

Following the main direction of the meridional flow the cyclonic motion is accumulated near the rotation axis. At low heating the cyclonic flow occupies a small domain close to the bottom, and the anticyclonic flows dominates in the upper layer (see Fig. 6(b)). The increase of Gr_f leads to a substantial growth of the cyclonic velocity maximum (from 0.2 mm/s to 7 mm/s) and weak changes of anticyclonic velocity maximum (about 1 mm/s), compare panels (b) of Figs. 6-7. The cyclonic flow at high values of Gr_f completely occupies the central part of the layer, spreading narrow wings along the bottom up to the

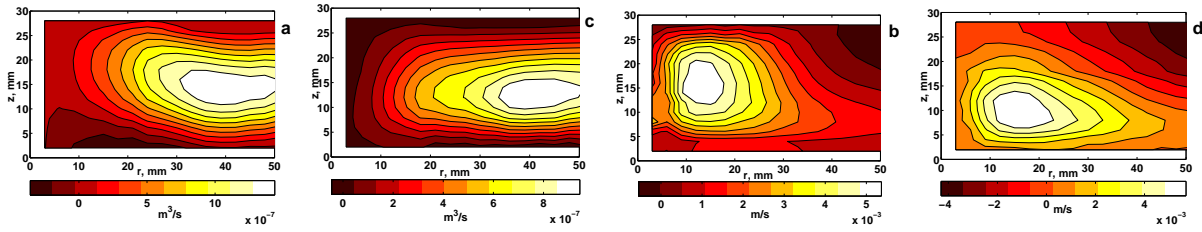


Figure 8. (Color online.) Stream function of the meridional mean velocity field (a,c) and mean azimuthal velocity field (b,d) for indirect circulation at $Gr_f = 9.1 \cdot 10^6$ and different rotation speed: a,b - $\Omega = 0.046 \text{ s}^{-1}$, c,d - $\Omega = 0.161 \text{ s}^{-1}$. Only the domain above the heater II is shown.

periphery. The anticyclonic flow is pushed towards the side wall.

The second important factor defining the flow structure is the speed of the frame rotation. Its influence is illustrated in Fig. 8, where the velocity fields for the central part of the layer, mostly occupied by cyclonic vortex, are shown for $Gr_f = 9.1 \cdot 10^6$ and two different values of the rotation speed - $\Omega = 0.046$ ($E = 0.066$) and $\Omega = 0.161 \text{ s}^{-1}$ ($E = 0.019$). The growth of the frame rotation speed leads to some decrease in intensity of the meridional circulation (see panels (a) and (c) of Fig. 8) because the increase of the background rotation suppresses the vertical motions. The azimuthal velocity fields for these two Ω are shown in Fig. 8(b,d). At a higher value of Ω the cyclonic flow is confined in the lower part of the layer.

5 Integral characteristics of differential rotation

The preceding results show that meridional circulation in both directions leads to a pronounced DR. The direct circulation initiates a strong cyclonic flow near the free surface at middle radii. The anticyclonic flow in this regime is localized near the bottom of the vessel and is weakened with increasing heating power. The result of indirect circulation is not quite symmetric. In this case, the cyclonic and anticyclonic flows are better separated in radial direction – the cyclone dominates in the central (polar) part of the layer, spreading at high values of heating power throughout the entire layer depth, while the anticyclone occupies the upper part of the periphery.

To quantitatively estimate the balance between the cyclonic and anticyclonic motions, we calculated the integral angular momentum for the whole layer; more precisely, for the whole area available for PIV measurements. Specifically, we calculated the relative variation S of the integral momentum L relative to the solid body rotation momentum of the layer L_s defined as "global super-rotation" (Read 1986)

$$S = \frac{L - L_s}{L_s}, \tag{5}$$

where

$$L = \int_{\delta_1}^{h-\delta_2} dz \int_{\delta_3}^{R-\delta_4} r dr \int_0^{2\pi} r v_\phi d\phi, \tag{6}$$

$$L_s = 2\pi \int_{\delta_1}^{h-\delta_2} dz \int_{\delta_3}^{R-\delta_4} \Omega r^3 dr, \tag{7}$$

and δ_i are the thickness of the boundary layers which are not accessible for PIV measurements. The results obtained for different values of Gr_f and a given rotation speed are shown in Fig. 9. The sign of the global angular momentum is directly related to the heating mode: peripheral heating provides the direct circulation that leads to the growth of the integral angular momentum of the fluid layer. On average, the fluid layer rotates faster than the background; therefore, this is a case of super-rotation. The maximum value of S achieved in the experiment is about 0.4. In contrast, central heating provides the indirect circulation that reduces the integral angular momentum; on average the layer rotates more slowly than the background (sub-rotation). Note that the increase in angular momentum at direct circulation is much

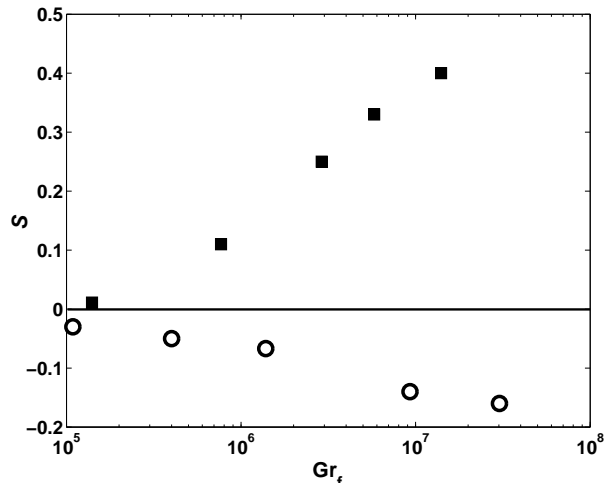


Figure 9. Global super-rotation S versus Gr_f for direct cell (squares) and indirect cell (circles) circulation, $\Omega = 0.069s^{-1}$.

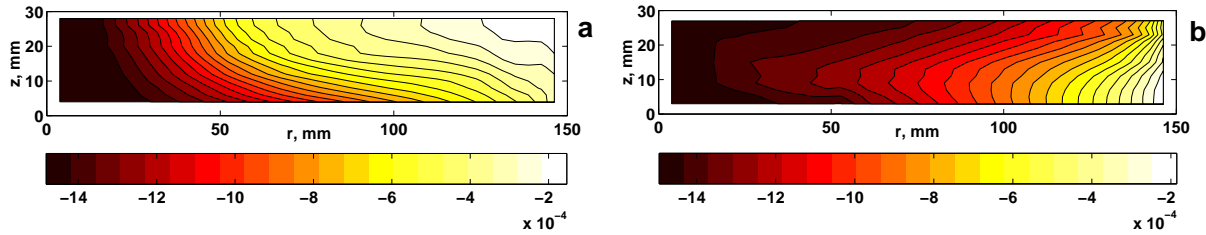


Figure 10. (Color online.) Local super-rotation s : (a)– direct circulation for $Gr_f = 1.4 \cdot 10^7$, $E = 0.032$; (b)– indirect circulation for $Gr_f = 3.02 \cdot 10^7$, $E = 0.032$.

greater than its decrease at indirect circulation for the same value of the heating power. The lowest value of S in the case of the indirect cell was $S \approx -0.16$.

Useful information might give the so-called "local super-rotation" s (Read 1986), defined as

$$s = \frac{v_\phi r}{\Omega R^2} - 1. \tag{8}$$

It shows the excess of angular momentum in comparison with highest possible angular momentum of the fluid element in a solid-body rotation state. The distribution of s for different types of meridional circulation is shown in Fig. 10. This figure shows that even for high values of Grasshoff number the local super-rotation s is negative everywhere (sub-rotation). Note, that numerical simulation in case of stress-free sidewalls showed that there is noticeable area with $s > 0$ (Read 1986). This proves the strong influence of the side wall boundary conditions on the distribution of angular momentum.

Angular momentum redistribution in the fluid layer occurs due to the action of net torque due to friction at the bottom and side walls (the upper surface can be considered stress-free, and the torque on the upper surface is negligible). In the case of direct meridional circulation the anticyclonic flow in the lower layer generates torque that injects angular momentum into the layer. Meridional flow provides the transfer of angular momentum from the lower to upper part of the layer. The sink of the angular momentum occurs in the viscous boundary layers occupied by the cyclonic flow. In the case of an indirect cell the sink of the angular momentum is located in the central part of the bottom occupied by an intensive cyclonic vortex, and the source of the angular momentum is located at the upper part of the side wall - the area of anticyclonic flow.

Thus, the flow structure and the imbalance between cyclonic and anticyclonic motion observed in the experiment is a consequence of different boundary conditions: non-slip on rigid boundaries, and stress-free on the surface. This agrees with general conclusions made from numerical simulations (Williams 1968) and (Read 1986).

Table 2. Grasshoff number and the parameter Q for all experiments

Gr_f	$1.4 \cdot 10^5$	$7.7 \cdot 10^5$	$2.9 \cdot 10^6$	$5.8 \cdot 10^6$	$1.4 \cdot 10^7$
Q	0.0082	0.0066	0.0066	0.0063	0.007

Note that some discrepancies exist between our experimental results and the analysis of the azimuthal circulation made in (Read 1986), where the flow structure analysis was made through dimensionless parameter Q which was defined using the aspect ratio, Ekman number and Rayleigh number Ra ,

$$Q = \text{Ra}^{-1/2} E^{-1} \varepsilon^{-3/2}, \quad (9)$$

$$\text{Ra} = \frac{g\beta L^3 \Delta T}{\chi \nu}, \quad (10)$$

where L is the horizontal length scale and ΔT is the horizontal temperature drop. Q describes the ratio between thickness of thermal boundary layer (non-rotating) and that of the Ekman boundary layer. It was shown that global super-rotation depends on Q in the follow way: the super-rotation is almost constant for slow rotation ($Q < (\varepsilon/\text{Pr})^2$); it increases at moderate rotation ($(\varepsilon/\text{Pr})^2 Q < 1$), and it decreases quickly at rapid rotation ($Q > 1$). Calculating Q for all measured experimental regimes (taking $L = R$), we found that Q changes very weakly (see Table 2). Thus, the whole variety of observed regimes exist under similar values of Q and belong to the case of "moderate" rotation.

The independence of Q on Gr_f can be easily understood if we expand the expression for Q and rewrite it in the following form

$$Q = 2\Omega \left(\frac{h}{g\beta\Delta T} \cdot \frac{1}{\text{Pr}} \right)^{1/2}. \quad (11)$$

In our experiments, all parameters from (11) except Pr and ΔT were constant. The growth of Gr_f leads to an increase of the mean temperature of the fluid T and ΔT , but to the decrease in the value of Pr . The decrease of Pr with growth of T is caused by strong temperature dependence of oil viscosity ν . As a result $(\text{Pr}\Delta T)^{-1/2}$ and parameter Q are almost independent of Gr_f . Note that the simulations of Read (1986) were performed for $\varepsilon = 1$, $\text{Pr} = 10$, a fixed temperature drop (heating) and varying Ekman number. In our experiments, the aspect ratio was smaller ($\varepsilon = 0.2$), the Prandtl number an order of magnitude larger, the rotation speed fixed. The heating power was the main governing parameter, which provided the variety of regimes.

As previously stated, the structure of the meridional flow is different at direct and indirect circulations (compare Fig. 5,a and Fig. 7,a). To estimate the energy balance, we compared the total energy of the meridional flow W_r for different kinds of circulation. Our measurements showed that the energy of the indirect meridional flow (provided by heater II) is about two times higher than the energy of the direct circulation (provided by heater I) for the same heating power. Therefore, for comparison of the energy budgets of the direct and indirect cells we used the Grasshoff number Gr_f and plotted the energy of the meridional circulation versus Gr_f . Fig. 11 shows that despite different structures of meridional circulation for the direct and indirect cells W_r for both cells is well correlated with the Grasshoff number. The function $W_r(\text{Gr}_f)$ is given in log-log scale and displays a power law close to "1/2".

We then analyzed how the energy of the cyclonic and anticyclonic motions W_c and W_a depend on the type of circulation and on the Grasshof number. Direct circulation results in a much more intensive cyclonic flow – than indirect circulation at the same Gr_f . However, in spite of the great difference in the structures and intensities of the cyclonic flow in the direct and indirect cells the dependence of W_c on the Grasshoff number is similar in both cases (see Fig. 12, where the energy of the cyclonic motion is shown versus the Grasshoff number for both circulations).

We could not obtain a similar picture for anticyclonic flow, because in the case of direct circulation the anticyclonic motion is mainly located in the boundary layer and could not be reconstructed with sufficient

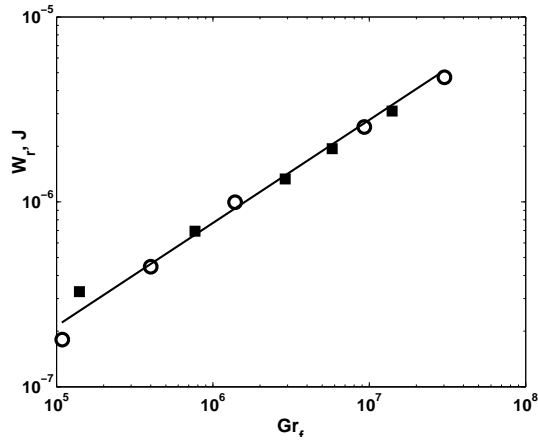


Figure 11. Total energy of the meridional flow versus Grasshoff number for direct (squares) and indirect (circles) circulation, $\Omega = 0.069s^{-1}$. The solid line shows the slope for $W_r \sim \sqrt{Gr_f}$.

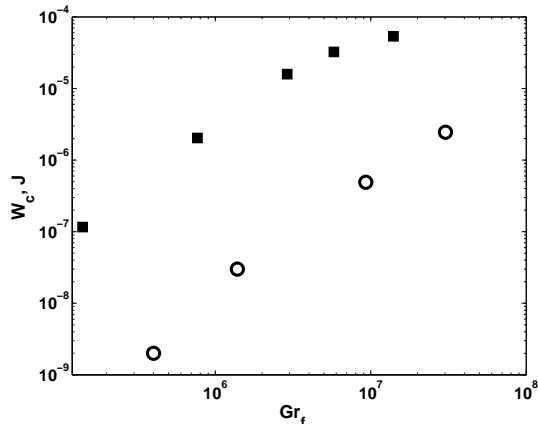


Figure 12. Total energy of the cyclonic flow at direct (squares) and indirect (circles) circulation versus the Grasshoff number, $\Omega = 0.069s^{-1}$.

accuracy. Fig. 13 shows the ratio of the cyclonic to anticyclonic flow energy for the indirect circulation. From this graph it is evident that in the considered range of parameters, this ratio grows linearly with the Grasshoff number. Thus, if this tendency remains valid at higher values of Gr_f , the energy of the cyclonic flows will surpass the energy of the anticyclonic flow at $Gr_f > 2 \cdot 10^7$.

Finally, we considered the direct characteristics of differential rotation. Note that DR is one of the major mechanisms of magnetic field generation in cosmic bodies; namely, DR is responsible for generation of the toroidal (azimuthal) magnetic field from the poloidal field. The efficiency of this mechanism depends on the gradient of the azimuthal velocity. The nondimensional characteristic of a dynamo process based on DR – the so-called "dynamo number" includes some characteristic value of the gradient of the mean azimuthal velocity (in the radial or meridional direction) in the domain where the dynamo action is localized (Zeldovich *et al.* 1983). Since we studied the DR outside a special dynamo problem, we use, as characteristics of DR, the mean values of the gradients $\partial_r v_\phi$ and $\partial_z v_\phi$ calculated over the domain of reconstruction.

$$D_r = 2\pi \int_{\delta_1}^{h-\delta_2} dz \int_{\delta_3}^{R-\delta_4} r(\partial_r v_\phi) dr, \tag{12}$$

$$D_z = 2\pi \int_{\delta_1}^{h-\delta_2} dz \int_{\delta_3}^{R-\delta_4} r(\partial_z v_\phi) dr. \tag{13}$$

The results are shown in Fig. 14 as functions of the Grasshoff number for both circulations. Panel (a) of

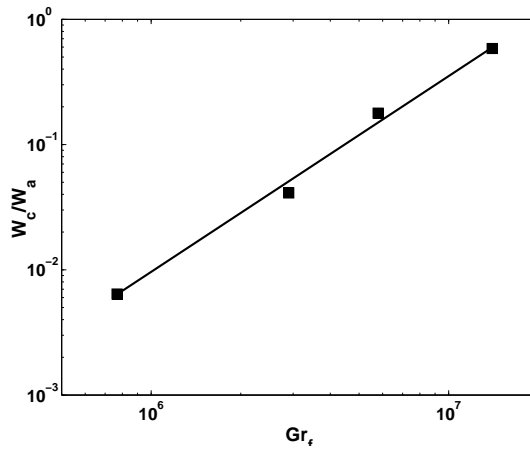


Figure 13. Ratio of the cyclonic motion energy to the energy of anticyclonic motion under indirect circulation, $\Omega = 0.069s^{-1}$.

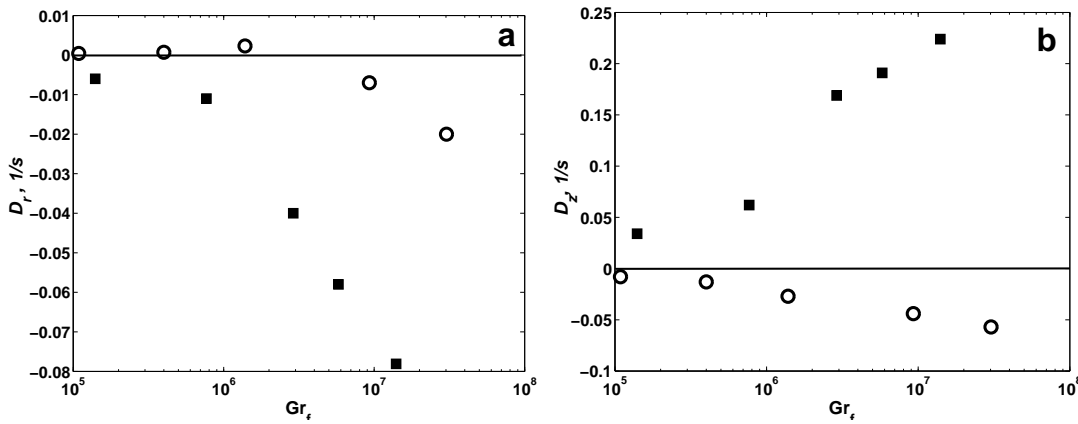


Figure 14. Mean radial D_r (a) and vertical D_z (b) gradients of azimuthal velocity for direct (squares) and indirect (circles) circulation versus the Grasshoff number for, $\Omega = 0.069s^{-1}$.

this figure shows that the mean radial gradient is negative for direct circulation (the central part rotates faster than the periphery), and that its value grows with the Grasshoff number. For indirect circulation, the mean radial gradient is close to zero at low Grasshoff number (the cyclonic and anticyclonic motions are separated vertically, but not radially) and becomes negative at high Gr_f . Then, the radial DR is weaker as in case of direct circulation, but the central part also rotates faster than the periphery. The behavior of the mean vertical gradient is quite different for two circulations: a positive vertical gradient increases with a growing Grasshoff number (approximately as $\log(Gr_f)$) at direct circulation, whereas a weak negative gradient characterizes the indirect circulation.

6 Summary

We studied the formation of DR for direct and indirect meridional cells. In the case of a direct cell, the cyclonic flow prevails and spans nearly the entire layer except for a relatively small zone at the periphery near the bottom. The indirect cell is characterized by competition between the cyclonic flow in the central part and anticyclonic flow at the periphery. The ratio W_c/W_a grows with Gr_f and approaches unity at $Gr_f \approx 2 \cdot 10^7$.

The structure of azimuthal flows and their intensities are determined by the difference between friction force torques at the rigid boundaries and the free surface. The condition of a steady-state regime is zero net torque. Torque due to frictional forces at the solid boundaries serves as a source of the angular momentum in the anticyclonic flow area and as a sink in the cyclonic flow area. During transition to a steady-state

regime the net torque is nonzero and leads to variation in overall angular momentum. Direct circulation leads to the growth of overall angular momentum, whereas indirect circulation causes it to decrease. At the same Gr_f the increase in angular momentum at direct circulation is much stronger than its decrease at indirect circulation.

DR is caused by the meridional transport of angular momentum. We have shown that the energy of the meridional circulation grows with the Grasshoff number as $\sqrt{Gr_f}$ at both directions of circulation. We characterize the differential rotation by the mean values of radial and vertical gradients of the azimuthal velocity. Direct circulation provides a strong negative mean radial gradient, which means that the central part rotates faster. The same tendency exists at indirect circulation, but the gradient is much smaller or even close to zero at low Grasshoff numbers. Direct circulation gives rise to a pronounced vertical gradient (positive), which grows with Grasshoff number. Indirect circulation provides a weak negative gradient. This difference follows from the very structure of the flow: direct circulation provides a large cyclonic area localized above the anticyclonic flow, and indirect circulation leads to substantial separation of these two area in the radial direction (the cyclonic flow is localized close to the rotation axis and the anticyclonic flow is concentrated near the side wall).

Acknowledgment

Financial support from RFBR under grants 07-01-92160 and 07-05-00060 is gratefully acknowledged.

REFERENCES

- Ya.B.Zeldovich, A.A.Ruzmaikin, and D.D.Sokoloff. Magnetic Fields in Astrophysics. Gordon and Breach Science, New York, 1983.
- L.L.Kitchatinov and G.Rudiger. Stability of toroidal magnetic fields in the solar tachocline and beneath. *Astron.Nachr.* 328, 1150-1154, 2007.
- N. Kleeorin and I. Rogachevskii. Effect of heat flux on differential rotation in turbulent convection. *Phys. Rev. E* 73, 046303, 2006.
- G.P.Williams. Thermal convection in a rotating fluid annulus: part 2. Classes of axisymmetric flow. *J. Atmos.Sci.* 24, 162-174, 1967.
- G.P.Williams. Thermal convection in a rotating fluid annulus: part 3. Suppression of the frictional constraint on lateral boundaries. *J. Atmos.Sci.* 25, 1034-1045, 1968.
- P.Highnett, A.Ibbetson and P.D.Killworth. On rotating thermal convection driven by non-uniform heating from below. *J.Fluid.Mech.* 109, 161-187, 1981.
- B.M.Boubnov, G.S.Golitsyn. Convection in Rotating Fluid. Kluwer Academic, Dordrecht and Boston, 1995.
- R.Hide. An experimental study of thermal convection in rotating liquid. *Phil.Trans.Roy.Soc.London* 250, 442-478, 1958.
- D.Fultz and J.A.C.Kaiser. The disturbing effects of probes in meteorological fluid-model experiments. *J. Atmos.Sci.* 28, 1153-1164, 1971.
- T.W.Spence and D.Fultz. Experiments on wave-transition spectra and vacillation in an open rotating cylinder. *J. Atmos.Sci.* 34, 1261-1285, 1977.
- M.J.S. Belton, G.R. Smith, G.Schubert, and A.D. Del Genio. Cloud patterns, waves and convection in the Venus atmosphere. *J.Atmos.Sci.* 33, 1394-1417, 1976.
- P.J.Gierasch. Meridional circulation and the maintenance of the Venus atmospheric rotation. *J.Atmos.Sci.* 32, 1038-1044, 1975.
- G.Shubert and R.E.Young. The 4-day Venus circulation driven by periodic thermal forcing. *J. Atmos.Sci.* 27, 523-528, 1970.
- W.B.Rossow. A general circulation model of Venus-like atmosphere. *J.Atmos.Sci.* 40, 273-302, 1983.

- P.L. Read. Super-rotation and diffusion of axial angular momentum: II. A review of quasi-axisymmetric models of planetary atmospheres. *Quart J.R.Met.Soc.* 112, 253-272, 1986.
- P.L. Read. Super-rotation and diffusion of axial angular momentum: I. "Speed limits" for axisymmetric flow in a rotating cylindrical fluid annulus. *Quart J.R.Met.Soc.* 112, 231-252, 1986.
- G.P.Bogatyrev. Excitation of a cyclonic vortex or a laboratory model for a tropical cyclone. *Pisma Zh.Eksp. Teor. Fiz.* 51, 557-559, 1990.
- G.P.Bogatyrev and B.L.Smorodin. Physical model of the rotation of a tropical cyclone. *Pisma Zh.Eksp. Teor. Fiz.* 63, 25-28, 1996.
- G.P.Bogatyrev, I.V.Kolesnichenko, G.V.Levina, and A.N.Sukhanovsky. Laboratory model of generation of a large-scale spiral vortex in a convectively unstable rotating fluid. *Izvestiya Atmospheric and Oceanic Physics* 42, 423429, 2006.
- Boubnov B.M. and van Heijst G.J.F. Experiments on convection from a horizontal plate with and without background rotation. *Exp.in Fluids* 16, 155-164, 1994.
- M.Raffel, C.Willert, J.Kompenhans. Particle Image Velocimetry: A Practical Guide. Berlin: Springer, 1998.
- Ke-Qing Xia , Chao Sun, and Sheng-Qi Zhou. Particle image velocimetry measurement of the velocity field in turbulent thermal convection. *Phys. Rev. E* 68, 066303, 2003.